International Journal of Modern Manufacturing Technologies
ISSN 2067–3604, Vol. XVII, No. 2 / 2025
https://doi.org/ 10.54684/ijmmt.2025.17.2.81

SYNTHESIS OF HARD CARBON ANODE FROM BIO-WASTE OF HEMP LEAVES FOR SODIUM-ION BATTERIES

Elendu Ekwueme Samson[1], Eris Elianddy Supeni[1], Mohd Khairol Anuar Mohd Arffin[1], Suhadi Shafie[1], Muhammad Ishaq[2]

[1]Department of Mechanical & Manufacturing Engineering, Facuty of Engineering, Universiti Putra Malaysia, 43400 UPM Serdang Selangor Darul Ehsan, Malaysia
[2]School of Chemistry and Chemical Engineering, Shanghai Electrochemical Energy Device Research Center Shanghai Jiao Tong University Shanghai, China

Corresponding author: Eris Elianddy Supeni, eris@upm.edu.my

Abstract: As societies worldwide strive to mitigate the impacts of climate change and transition towards renewable energy sources, the need for reliable and scalable energy storage systems has become increasingly pronounced. This trend reflects a broader shift towards the adoption of clean energy technologies, driven by the imperative to reduce greenhouse gas emissions and secure a sustainable future for generations to come. Against this backdrop, research efforts have intensified to innovate and optimize energy storage materials and devices, with a particular emphasis on enhancing performance metrics such as energy density, cycling stability, and cost-effectiveness. Among the various energy storage technologies, the prominence of batteries, supercapacitors, and other electrochemical energy storage systems has grown significantly, owing to their versatility, scalability, and applicability across diverse sectors, including transportation, grid management, and portable electronics. Moreover, the exploration of novel materials and synthesis techniques holds promise for further advancing the capabilities of these energy storage technologies, paving the way for more efficient and sustainable energy storage solutions. In this context, the utilization of renewable and biowaste-derived materials presents an attractive avenue for achieving both environmental sustainability and technological innovation. Harnessing the abundant resources offered by nature, such as hemp leaves, for the synthesis of advanced carbon materials underscores the potential of bio-inspired approaches in addressing the pressing challenges of energy storage. By aligning with the principles of circular economy and resource efficiency, such initiatives contribute to the realization of a cleaner, greener energy landscape that is essential for sustainable development goals. The study investigates the impact of synthetic conditions, particularly post-HCl treatment and water washing, on the electrochemical storage capability of Na-ions. Electrochemical results reveal that HLHC subjected to post-water washing demonstrates superior performance compared to those treated with HCl. Specifically, the HLHC-13 (water-washed) and HLHC-13 (HCl-treated) anodes exhibit initial specific capacities of 303.2 and 277.7 mAh g-1 for the first charge process, and 384.79 and 368.3 mAh g-1 for the first discharge process, respectively. This results in initial Coulombic efficiencies (ICE) of 81.0 % and 75.3 %, respectively. Furthermore, both variants display remarkable reversible capacity retention, ICE, and rate capability.

Key words: Sodium-ion batteries (NIBs), electrochemical energy storage (EES), hard carbon (HC), hemp leaves (HL).

1. INTRODUCTION

Sodium-ion batteries (NIBs) are regarded as the most promising electrochemical energy storage (EES) technologies of the future generation for high-tech electric vehicles, portable electronics, and grid-scale energy storage applications due to their abundant global sodium resources and inexpensive cost [1]. To achieve the practical implementation of NIBs, significant endeavors have been devoted to the exploration of compatible electrode materials that can support consistent cycling and sufficient reversible capability. Non- graphitizable hard carbon (HC) is widely regarded as the most promising anode material for NIB technology on account of its economic cost and exceptional capacity to store Na-ions [2].HC is a potential anode material that outperforms graphite in terms of capacity and cycling stability due to its unusual house-of-cards microstructure and high level of disordered graphene sheets, which enable multiple Na-ion storage mechanisms, including intercalation, nanopore filling, and surface chemisorption[3]. Researchers in both academia and industry have started using plant leaf biomass as an energy source for electrochemical energy storage (EES) and conversion since it is the most abundant, biodegradable, and ecologically friendly carbon source on the planet [4]. HC obtained from natural leaves functions as an anode for Na-ion storage [5]. It possesses a comprehensive carbonaceous framework featuring integrated channels and porous architectures that are substantially hierarchical

(micro/nanopores). These features enhance the kinetics of charge transfer and provide an effective backdrop for the swift movement of ions and electrons [6][7]. Indeed, it has been shown that a multitude of HC anode materials derived from biowaste possess exceptional ICEs and a commendable ability for storing Na-ions [8]. Significantly, by examining the historical progression of HC synthesis obtained from biomass, one can gain insight into the overarching considerations associated with acid-base therapy during various phases of HC development.

2. MATERIALS AND METHODS

2.1. Materials synthesis

Using an 800G 3000W miller, the hemp leaves (HL) were first ground and sieved into particles smaller than 1 mm. They were then subjected to an hour-long ultrasonic treatment in deionized (D.I.) water, filtered, cleaned, and freeze-dried for a whole day. After that, the precursor was subjected to pyrolysis in a tabular furnace (OTF-1600X) set at temperatures of 1100, 1300, and 1500 °C for a duration of 1 hour under an Ar stream, with a heating rate of 5.°C min-1. After that, it was allowed to cool down to room temperature naturally. Based on the carbonization temperature, the prepared samples were denoted as HLHC-11, HLHC-13, and HLHC-15. The electrochemical performance was optimized by treating the pyrolyzed sample with two distinct solvents, for instance, HLHC-13. To prepare the sample treated with DI water, the HLHC-13 was first immersed in the solution overnight at 80 °C, filtered, rinsed, and then freeze-dried. In the same way, the sample that was treated with HCL was prepared by heating the HLHC-13 sample in a 1M HCL solution at 80 °C for a whole night, filtering it, and then washing it with DI water until its pH reached 6-7. Finally, it was freeze-dried for 24 hours. In the end, the HLHCs were ground by hand, sieved, and kept in a dry environment.

2.2. Material characterizations

The DX-2700BHX diffractometer and Cu Kα radiation (λ = 1.5406 Å, 45 kV, 40 mA) were used to obtain the X-ray diffraction patterns. A Nova Nano SEM 450 manufactured by FEI Company was used for field emission scanning electron microscopy (FE-SEM). A Micromeritics surface area analyzer was used to conduct nitrogen sorption analysis at 77 K. (model ASAP 2020). X-ray photoelectron spectroscopy (XPS) was carried out to analyze the elemental states and chemical composition of the prepared samples using Axis Ultra DLD and Kratos X-ray photoelectron spectroscopy.

2.3. Electrochemical measurements

Using a planetary mixer (THINKY) set at 2000 rpm, the slurry was blended, consisting of HLHC samples, a CMC binder, and super P (8:1:1 wt%) to create the working electrodes. The slurry was left to dry overnight under a vacuum at 120°C after being cast on foil made of battery-grade aluminum. A CR2025-type coin cell was meticulously built with the electrodes utilizing a Na-metal counter electrode and a glass fiber mat (GA 55, Advantech, Japan) as the separator in an Ar-filled dry glove box with oxygen levels less than 0.1 ppm. The electrolyte was composed of EC/DMC (1:1 by volume) with 1M NaPF6 and a 5% FEC addition. The galvanostatic model using a Neware battery test system (Shenzhen Xinwei Electronics Co., Ltd.) running at 25±1°Cwas used to cycle the cells tested. The voltage range was from 0.01to 2.5 V. A specific current of 200 mA g-1 is used in the definition of 1C. CV measurements (the potential range of 0.01 to 2.5 V vs. Na+/Na) and EIS (100 kHz to 0.01 Hz) of coin cells were tested on an electrochemical workstation (CHI660C, China), respectively.

3. RESULTS AND DISCUSSION

Hemp leaves-biowaste were utilized for our synthesis of hard carbon, hereinafter referred to as (HLHC). The synthesis process of HLHC is schematically illustrated in Figure 1(a), which includes simple grinding, washing, and freeze-drying of the precursor initially and is subjected to thermal pyrolysis at 1100–1500 °C, hereafter called HLHC-11, HLHC-1200 °C, HLHC-13, and HLHC-15 products. Detailed synthesis procedures are described in the experimental section. To find the influence of post-acid treatment on the electrochemical performance, the obtained HLHC pyrolyzed at 1300 °C, was first post-treated with two different solvents, such as HCl-leaching and D.I. water washing. The X-ray diffraction (XRD) patterns of the HLHC-13 (H2O/HCl-treated) samples, along with the associated precursor, are displayed in Figure 1(b). The XRD spectra of HLHC precursor (after freeze-drying/before pyrolysis) show a mixture of a broad and a small sharp crystalline diffraction peak of graphite at 2θ=21.2°can be attributed to a mixed phase of graphitic domains in the precursor sample. After being subjected to pyrolysis, two peaks observed with relatively broad diffraction angles of2θ

=22.8° and 43.6° correspond to the (002) and (100) Bragg reflections of graphitic domains [9], indicating that both the carbon samples have small layer-to-layer-crystalline-coherency with wider interlayer spacing between sp2 carbon sheets than 0.334 nm graphite layer

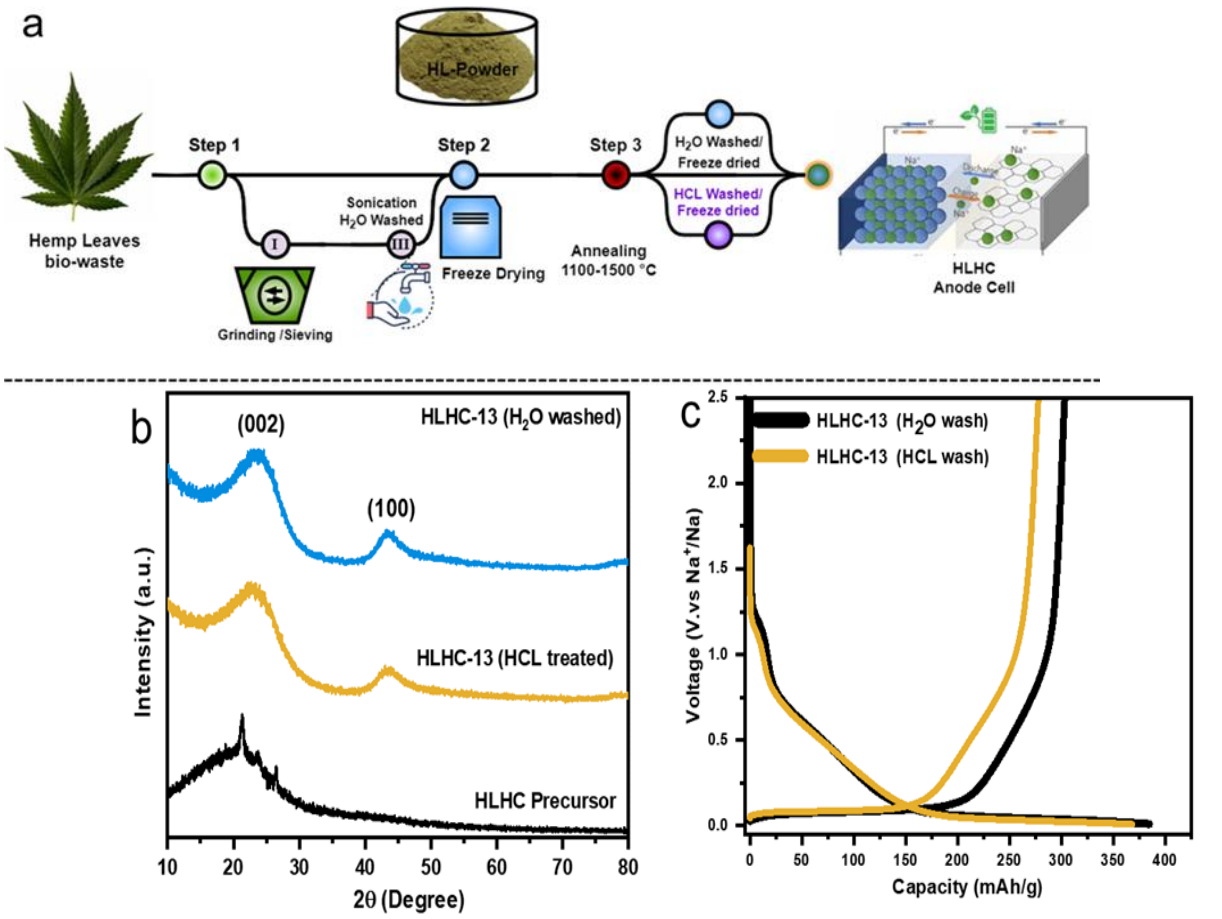

Fig. 1. (a) The schematic diagram for a workflow with a simpler branching model for hemp leaves derived hard carbon (HLHC). (b) Comparison of XRD patterns for the water-washed HLHC-13, and (c) acid-washed HLHC-13. (c) Initial charge-discharge curves of the Na cells for the corresponding HLHC-13 (H_2O wash) and HLHC-13 (HCL wash), respectively.

Since apparent differences between the two preparation methods are observed in the facile D.I water washing, based on this investigation, in the following section, the effect of temperature optimization on the structure and electrochemical properties of HLHC samples pyrolysis at 1100 °C, 1300 °C, and 1500 °C, followed by post-water washing, was treated. Figure 2(a-c) illustrates the low and high-resolution scanning electron microscope (SEM) images of HLHC-11, HLHC-13, and HLHC-15 samples after post-D. I water washing, respectively. SEM images show that all the HLHC samples offer highly hierarchical porous features with a large number of carbon nanosheets randomly intertwined with each other, forming macroscopic channels. These inherited macroporous channels from the Hemp leaves provide special access to the Na+-ion transportation yellow arrows) to the carbon nanosheets inside. Moreover, all the HLHC samples maintain their structural integrity even after being subjected to different high temperatures, indicating good mechanical and thermal stability.
Figure 2(d) shows the XRD data of HLHC-11, HLHC-13, and HLHC-15 samples after post-D. I will use water washing to verify the disordered structure information further. The XRD pattern of the HLHC samples shows two broad peaks at 2θ =22° and 43°, attributed to the (002) and (100) Bragg reflection planes of the typical amorphous carbon.

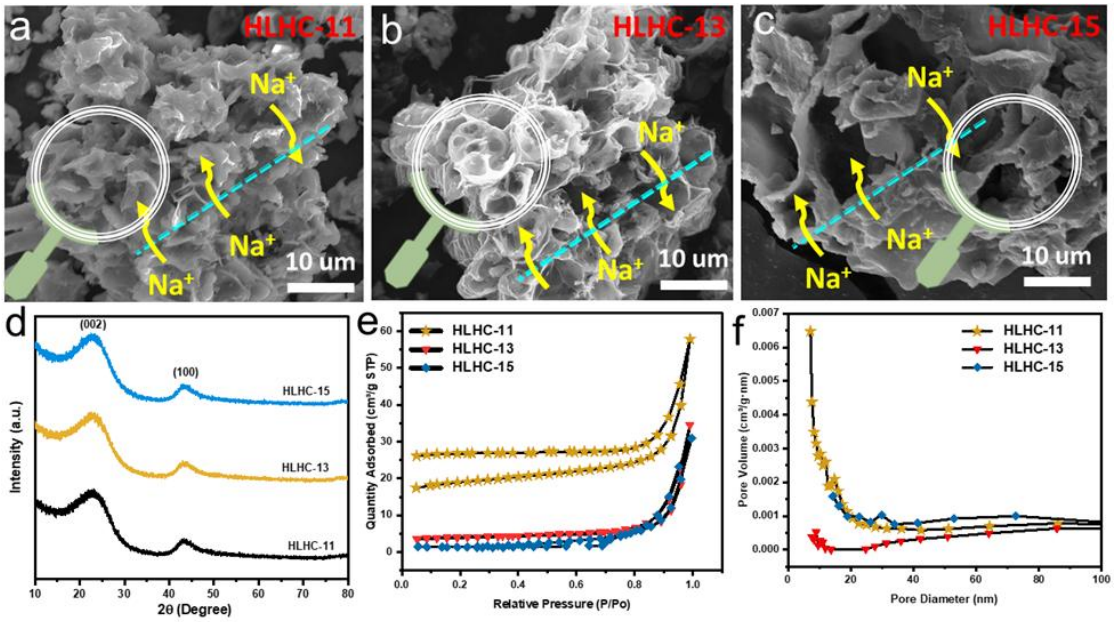

Fig. 2. High-resolution SEM images of (a,) HLHC-11, (b) HLHC-13, and (c) HLHC-15, samples after post D.I water washing, respectively. Structure elucidation and surface area characterization of the HLHC samples. (d) XRD patterns and (e, f) Nitrogen (N_2) adsorption/desorption isotherm of the HLHC-11, HLHC-13, and HLHC-15, samples after post D.I water washing

Table1. Physical parameters of the HLHCS samples from XRD and BET data

Sample	d_{002} [nm]	La[nm]	Lc [nm]	SBET [$m^2\ g^{-1}$]	Pore volume [$cm^3\ g^{-1}$]
HLHC-11	0.403	3.08	0.98	58.546	0.0895
HLHC-13	0.394	3.82	1.36	4.5001	0.0487
HLHC-15	0.384	3.96	1.40	5.675	0.0231

Comparatively, the (002) peaks shift faintly to a higher reflection angle, and the (100) peak intensity increases relatively when the pyrolysis temperature reaches 1500 °C, showing that the interlayer distance (d002) decreases and the degree of order increases. Based on Bragg's equation, the average interlayer distance (d002) was estimated to be 0.403, 0.394, and 0.384 nm for HLHC-11, HLHC-13, and HLHC-15 samples, respectively (as listed in Table 1). The d-spacing data show that even after being annealed at 1100 °C, the HLHC retains a highly disordered microcrystallite phase (>0.40 nm) and a somewhat ordered microcrystallite (pseudo-graphitic; >0.36-0.40 nm) phase at 1500 °C. These structures are ideal for Na+-ion storage because the energy barrier for inserting or extracting Na+-ion is minimal (close to 0eV) [11]. The N2 gas (77K) adsorption/desorption analysis was used to characterize the surface area (SA) and porosity of the HLHC samples. All the HLHC samples show type IIN2 isotherms corresponding to the adsorption/desorption of macroporous material, as shown in
Figure 2(e), the Brunauer–Emmett–Teller (BET) surface area (SA), pore volume (PV), and average pore sizes are summarized in Table 1. For the HLHC-11, the SA and pore volume are calculated to be 58.546 $m^2\ g^{-1}$ and 0.0895 $cm^3\ g^{-1}$. The SA and pore volumegradually decreases to 4.500 $m^2\ g^{-1}$ and 0.0487 $cm^3\ g^{-1}$ for HLHC-13, and 5.675 $m^2\ g^{-1}$ and 0.0231 $cm^3\ g^{-1}$ for HLHC-15, respectively. This low SA could result in inadequate SEI production and a high ICE [12]. The pore size distribution plot for all HLHC samples shows limited amounts of nanopores; most of the pores are in the range of macropores, Figure 2(f). The surface chemical composition and state of HLHC samples were investigated by XPS analysis. As shown in Figure 2(a), C 1s, N1s, and O 1s signals located at ~284.75 eV, ~401.0eV, and ~531.67 eV were detected in the XPS survey-scan spectra of all the HLHC samples, signifying the existence of C, N, and O elements without any other impurities.
The quantitative atomic percentages of C, N, and O are shown in Figure 3(b). The carbon contents in HLHC-11, HLHC-13, and HLHC-15 were 89.83 %, 86.31 %, 86.57 %, and 92.93 %, while the N contents were 1.09 %, 0.74 %, 0.4 %, and 0.27 %, respectively. It can be seen that the N content decreases as the carbonization temperature rises because high temperatures cause the N-C bond to break. Similarly, different surface O-abundances are found to be 9.83 % for HLHC-11, 12.95 % for HLHC-13, and 6.8 % for HLHC-15. It has been proposed that the oxygen-containing functional groups on the surface of carbon-based anodes contribute to their capacity at voltages greater than 1.5 V [229]. As shown in Figure 3 (c-e), the fitting curves of C1s spectra for all the samples can be deconvoluted into three symmetrical peaks at 284.75, 286.45, 289.2, and 292.82 eV are attributed to C-C/C=C (sp2, sp3), C=O, O-C=O, and π-π* bonds, respectively [12].

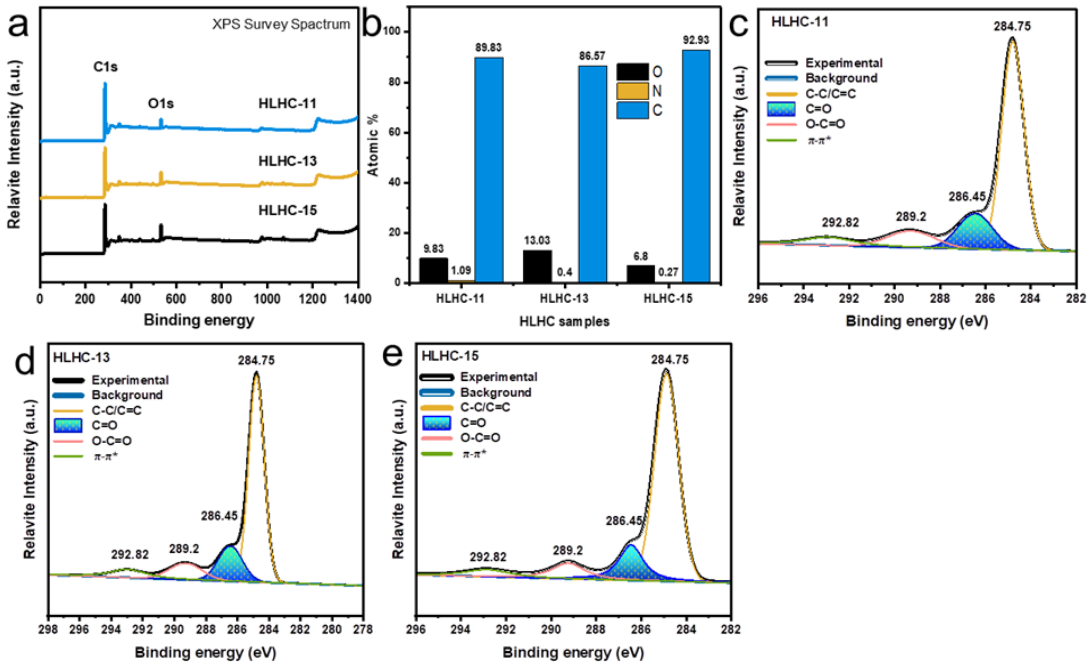

Fig. 1. (a) XPS survey spectra of HLHC-11, HLHC-13, and HLHC-15 samples (b) the corresponding quantitative atomic percentage of C, N, and O. XPS C1s photoelectron spectra of (c) HLHC-11, (d) HLHC-13, and (e) HLHC-15 samples.

4. CONCLUSIONS

In conclusion, a simple thermal pyrolysis method with post-facile water washing is reported to prepare HLHC. The influence of the synthetic conditions (i.e., post-HCL treatment and water washing) on the electrochemical Na+-ion storage performance was evaluated and compared initially. The electrochemical results revealed that HLHC prepared via facile post-water washing outperformed those treated by HCL and demonstrated excellent reversible capacity retention (99.12% after 100 cycles), excellent ICE (80 %), and rate capability (228 mAh g^{-1} at 1C). The synthesis method and leaves-bio waste precursor here provide eco-friendliness and readily scaled-up production of high-performance HLHC anode material for Na+-ion battery applications.

Author contributions: All authors contributed to the study conception and design. Data curation, investigation, methodology, validation, and initial draft writing were performed by Anish K Raj. Conceptualization, resources, supervision, visualization, review and editing were performed by Bikash Ranjan Moharana. Data curation, supervision, review and editing were performed by Kalinga Simant Bal. Supervision, review and editing were performed by Shaik Mozammil. All authors have read and agreed to the published version of the manuscript.

Funding source: The research received no specific grant from any funding agency.

Conflicts of interest: There is no conflict of interest

Acknowledgments: The author gratefully acknowledges financial support from Puncak RM Berhad University Community Transformation Center (UPM) and the immense contribution of Muhammad Ishaq to the success of this work.

REFERENCES

[1] Y. Gao, H. Zhang, J. Peng, L. Li, Y. Xiao, L. Li, Y. Liu, Y. Qiao, S.L. Chou, (2024), *A 30-year overview of sodium-ion batteries*, Carbon Energy, 6:e464, https://doi.org/10.1002/cey2.464

[2] H.R. Sarma, J. Sun, I.E. Gunathilaka, Y. Hora, M. Forsyth, N. Byrne, (2024), *Investigation of structural & interfacial properties of hard carbon electrodes from cotton snippets toward sustainable sodium-ion batteries*, Sustainable Materials and Technologies, 39, e00846, https://doi.org/10.1016/j.susmat.2024.e00846

[3] F. Xie, Z. Xu, Z. Guo, M.-M. Titirici, (2020), *Hard carbons for sodium-ion batteries and beyond*, Progress in Energy, 2(4), 042002, DOI 10.1088/2516-1083/aba5f5

[4] Beda, J.-M. Le Meins, P.-L. Taberna, P. Simon, C.M. Ghimbeu, (2020), *Impact of biomass inorganic impurities on hard carbon properties and performance in Na-ion batteries*, Sustainable materials and technologies, 26, e00227, https://doi.org/10.1016/j.susmat.2020.e00227

[5] H. Darjazi, L. Bottoni, H. Moazami, S. Rezvani, L. Balducci, L. Sbrascini, A. Staffolani, A. Tombesi, F. Nobili, (2023), *From waste to resources: transforming olive leaves to hard carbon as sustainable and versatile electrode material for Li/Na-ion batteries and supercapacitors*, Materials Today Sustainability, 21, 100313, https://doi.org/10.1016/j.mtsust.2022.100313

[6] Yadav, S.K. Martha, (2019), *Biomass Derived Hard Carbon as Anode Materials for Sodium Ion Batteries*, Master thesis, Indian Institute of Technology Hyderabad, available at: https://raiithold.iith.ac.in
[7] Mohit, S.A. Hashmi, (2024), *Hard carbon anode derived from pre-treated bio-waste sugarcane bagasse for high-capacity sodium-ion battery fabricated with bio-degradable porous polymer electrolyte*, Journal of Energy Storage, 83, 110694, https://doi.org/10.1016/j.est.2024.110694
[8] M. Thenappan, K. Mathiyalagan, M. Abdollahifar, S. Rengapillai, S. Marimuthu, (2023), *Structural and electrochemical properties of Musa acuminata fiber-derived hard carbon as anodes of sodium-ion batteries*, Energies, 16(2), 979, https://doi.org/10.3390/en16020979
[9] S. Wu, H. Peng, J. Xu, L. Huang, Y. Liu, X. Xu, Y. Wu, Z. Sun, (2024), *Nitrogen/phosphorus co-doped ultramicropores hard carbonspheres for rapid sodium storage*, Carbon, 218, 118756, https://doi.org/10.1016/j.carbon.2023.118756
[10] P. Yu, W. Tang, F.-F. Wu, C. Zhang, H.-Y. Luo, H. Liu, Z.-G. Wang, (2020), *Recent progress in plant-derived hard carbon anode materials for sodium-ion batteries: a review*, Rare Metals, 39(9), 1019-1033.
[11] Y. Aniskevich, J.H. Yu, J.Y. Kim, S. Komaba, S.T. Myung, (2024), *Tracking Sodium Cluster Dynamics in Hard Carbon with a Low Specific Surface Area for Sodium-Ion Batteries*, Advanced Energy Materials, 14(18), id.2304300, doi: 10.1002/aenm.202304300
[12] Nagmani, S. Manna, S. Puravankara, (2024), *Hierarchically Porous Closed-pore Hard Carbon as Plateau-dominated High-Performance Anode for Sodium-ion Batteries*, Chemical Communications, 22, available at: https://pubs.rsc.org/en/content/articlelanding/2024/cc/d4cc00025k

Received: August 16th, 2025 / Accepted: December 5th, 2025 / Paper available online: December 20th, 2025